Applied Scientific Research **51:** 291–296, 1993.
F.T.M. Nieuwstadt (ed.), Advances in Turbulence IV.

The Motion of Microbubbles in a Forced Isotropic and Homogeneous Turbulence

LIAN-PING WANG and MARTIN R. MAXEY
Center for Fluid Mechanics, Turbulence, and Computation
Box 1966, Brown University, Providence, RI 02912

Abstract. We have studied the concentration distribution of microbubbles in forced isotropic turbulence. An initially uniform concentration field is shown to evolve to a highly *intermittent* or *spotty* concentration distribution at long time due to the interactions of microbubbles with small-scale, intense, and coherent flow vortical structures. The maximum bubble concentration can be as large as 3,000 times the mean concentration and the local accumulations occur preferentially in the regions of high flow vorticity and low flow pressure. A quantitative measure of global nonuniformity in the concentration field is used to confirm that the preferential accumulation does follow Kolmogorov scaling, as opposed to the large-scale scaling commonly used for dispersion quantification.

Key words: microbubble transport – local accumulation – turbulence structures – inertial bias

1. Introduction

In this paper we present some results on the transport of spherical microbubbles by an unsteady and isotropic turbulent flow. While most recent work[1–2] has focused on particle dispersion which is dominated by fluid motion at large scales, we are interested in the interactions of microbubbles with small-scale flow structures, in particular the flow vorticity field. Such a viewpoint is related to the recent in-depth understanding of intense, intermittent, coherent vortical structures that have been observed in turbulence at dissipation-range scales.[3–5]

A general particle does not follow the trajectory of a fluid element or tracer particle because of the additional effects of particle/fluid inertia and external forces. In a mixing layer where unsteady but persistent, large-scale vortical structures exist, heavy particles tend to veer away from the vortex center due to the centrifugal effect, which leads to local accumulations of particles near the edge of the vortical regions. In such a case, the particle-vortex interaction enhances the transverse dispersion[6–7] but inhibits the mixing of particles.[8] Even stronger accumulation may occur when steady and persistent vortical structures are present in the flow.[9–10] For similar reasons, the notion of *inertial bias*[11] has been introduced for the motion of heavy particles in an unsteady turbulent flow where a range of flow scales co-exist. In general heavy particles accumulate preferentially in regions of low vorticity or high strain rate. This has been confirmed by the results from full numerical simulations for non-settling particles.[12] Recently, we have found, from full numerical simulations, that the local accumulations of heavy particles follow

Kolmogorov scaling, i.e., strongest accumulation takes place when the particle inertia response time is made comparable to the flow Kolmogorov scale.[13] The present work will focus on the motion of microbubbles. Intuitively one may expect microbubbles to accumulate preferentially in regions of intense vorticity. The degree of local accumulation, the flow scale most responsible for this process, and the role of pressure fluctuations will be analyzed quantitatively. Recent related experimental studies include bubble vortex-ring interactions[14] and measurements of average turbulence statistics in bubbly flows[15,16].

2. Flow Simulation and Bubble Equation of Motion

A homogeneous, isotropic, and stationary turbulent flow was generated by full numerical simulations following Ruetsch & Maxey.[5] Here only the flow field simulated on a 48^3 grid was considered. Our previous experience with heavy particles[13] indicates that the qualitative features of the local accumulation are the same for flows at higher grid resolution. The wavenumbers resolved in the simulation were $0 < k < 22.5$. Random forcing[5] was applied to low wavenumbers ($k < \sqrt{8}$) to maintain the flow.

TABLE I

The flow parameters from the simulation on 48^3 grid.

u_0	L_f	T_e	ϵ	η	τ_k	v_k	λ	Re_λ
16.6	2.030	0.083	2943	0.0617	0.0106	5.83	0.6525	31.0

Table I lists the flow parameters (from left to right): the rms fluctuating velocity, integral length scale, eddy turnover time, dissipation rate, Kolmogorov length, time, and velocity scales, Taylor microscale, and Taylor microscale Reynolds number. We note that the relative scale separation, T_e/τ_k, in the flow is about 8. Other details of the flow, such as energy spectrum, may be found elsewhere.[5,13]

In this study, microbubbles were treated as monodisperse, rigid spheres. Unless special precautions are taken small gas bubbles ($< 200\mu m$) in water will be contaminated by surfactants and will respond essentially as rigid spheres. The equation of motion for a microbubble is similar to that used by Maxey[10] with a slight modification for the added mass term according to Auton *et. al*,[17] which is written in nondimensional form as

$$\frac{d\mathbf{V}}{dt} = \frac{\left(\mathbf{u}(\mathbf{Y},t) - \mathbf{V} + \mathbf{Q}\right)}{\tau_b} + 3\frac{D\mathbf{u}}{Dt}, \tag{1}$$

where the bubble response time (the origin is fluid inertia from the added mass term) $\tau_b = m_F/(12\pi a\mu)$ and the bubble rise velocity in still fluid $Q = -2\tau \mathrm{g}$.

$\mathbf{Y}(t)$ is the position of the bubble and $\mathbf{V}(t) = d\mathbf{Y}/dt$; $\mathbf{u}$ is the flow velocity field; a is the microbubble radius; m_F is the mass of the displaced fluid; μ is the dynamical viscosity of the surrounding fluid; and $\mathbf{g}$ is the gravitational acceleration. The two derivatives, d/dt and D/Dt, represent the rate of change following a moving bubble and a fluid element at the bubble location. The linear Stokes drag, buoyancy force, the force due to fluid element acceleration in the undisturbed flow field, and the added mass effect are included in the equation of the motion. Some test computations were made with a lift force, of the form discussed in Auton *et. al*,[17] included but this did not make a major qualitative change to the results presented here. Our aim is to understand the simpler dynamics of bubble motion represented here. A problem for *dirty* microbubbles is that the exact form of the lift force is still in question. Auton's result applies to clean bubbles where an inviscid flow description can be used.

In the simulation a statistically stationary flow velocity field was first generated in the same manner as Ruetsch & Maxey.[5] Next $131,072$ (N_p) microbubbles were introduced randomly into the flow at a reference time $t = 0$ with a uniform distribution in their location and the initial velocity equal to $\mathbf{Q}$. The location and velocity of each microbubble were then advanced simultaneously with the flow simulation. A fourth-order Adams-Bashforth method was used to integrate the microbubble equation of motion. The fluid velocity and acceleration at the location of a microbubble were interpolated from the values at neighboring grids using a partial Hermite scheme.[18]

3. Results and Discussions

The concentration, C, at any grid point is defined as the number of microbubbles found inside a small cube with its center at the grid point and its side equal to the grid spacing. Therefore it may take a value of zero or a positive integer. The concentration distribution is uniform at $t = 0$ but becomes more and more nonuniform as time increases. We found after about $2T_e$ the concentration field roughly reaches the asymptotic state which represents a balance between the local accumulation in coherent vortical structures at small scales and random, unsteady flow stirring at larger scales. The mean concentration averaged over space was $131,072/48^3 = 1.1852$.

In Fig. 1 we present a typical concentration field along with the flow enstrophy and pressure field on a slice from the 3-D simulation box. The concentration field is markedly *spotty* or *intermittent*. A maximum bubble concentration of 3,000 times the mean concentration has been observed in this simulation. Visually it is observed that bubbles stay preferentially in the regions of high vorticity and low flow pressure. Fig. 2(a) shows the average concentration versus the local flow enstrophy on those grid points where the local pressure fluctuation, $p = (P - < P >)/(\rho_f u_0^2/2)$, is specified. The results were averaged over ten time stations. In spite of the statistical uncertainties, it is seen that for a given level of p,

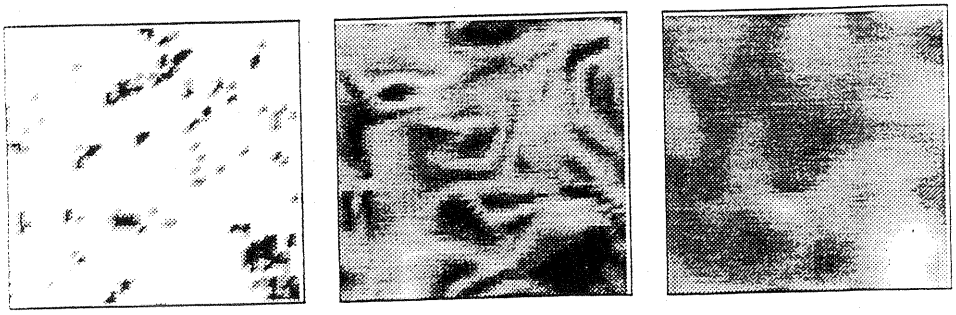

Fig. 1. Grey level plots of the microbubble concentration field (left), the flow enstrophy field (middle), and normalized fluctuation pressure field (right) at $t = 0.216$ in the plane $x_2 = 17L/48$. The highest grey level denotes at least twice the corresponding field mean for the first two quantities. For the p field the highest grey level represents regions of p no less than three times of the rms value and the lowest grey level (white) for p no larger than minus three times of the rms value. Microbubble parameters are $\tau_b/\tau_k = 1.0$ and $|\mathbf{Q}|/v_k = 1.0$. The gravity is pointing in the $-x_3$ direction.

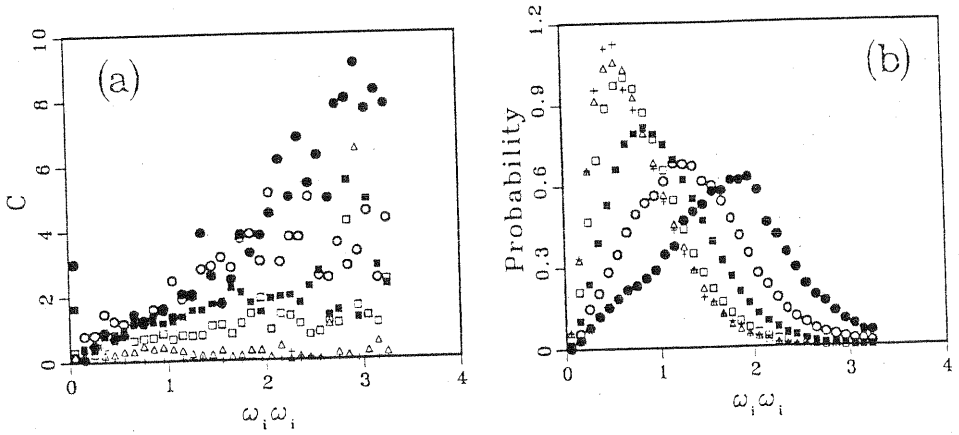

Fig. 2. (a) Correlation between the bubble concentration and the enstrophy conditioned by the pressure fluctuation. (b) The pdf distributions of enstrophy conditioned by the pressure fluctuation. Symbols: •, $-3 < p < -2$; ○, $-2 < p < -1$; ■, $-1 < p < 0$; □, $0 < p < 1$; △, $1 < p < 2$; +, $2 < p < 3$.

larger C is correlated with larger enstrophy. In addition, the correlation (or slope) decreases as p increases. On the other hand, for a given level of enstrophy, the mean concentration increases with decreasing p. Therefore, bubbles accumulate preferentially in the regions of either low pressure or high vorticity, and most likely in the regions of both low pressure and high vorticity, since in general pressure and vorticity fluctuations are correlated. This is shown by the conditional probability distributions of enstrophy in Fig. 2(b). For lower, negative pressure fluctuations the pdf is broader and corresponds to the larger enstrophy fluctuations. These

observations are of practical significance for cavitating flows. Gas microbubbles often act as cavitation nuclei and their trapping within strong vorticity regions coupled with the lower ambient pressure will tend to promote cavitation.

To find out when the strongest accumulation occurs, we introduce a probability density function of finding the concentration at a grid point equal to a particular value, denoted by $P_c(C)$. For the typical simulation shown in Fig. 1 $P_c(C=0) = 0.903$, indicating that about 90% of grid points have no bubbles, as compared to 31% for a uniform concentration. In addition $P_c(C \leq 10) = 0.982$ while only about 18% of bubbles are found at those grid points with $C \leq 10$. This means that most of the bubbles are located at a few grid points in space where the concentration is extremely high. A global measure of the degree of local accumulations may be defined as the integrated square deviation of the pdf relative to the value for a uniform concentration field (which can be determined exactly), $D_c = \sum_{c=0}^{N_p} \left(P_c(C) - P_c^u(C) \right)^2$. This global measure is found to reach a maximum when $\tau_b/\tau_k \approx 1$, which suggests that the Kolmogorov scale is the most important scale for the local bubble accumulation, as opposed to the energy-containing scales commonly used for dispersion quantification. It was found that the global measure only weakly depend on $|\mathbf{Q}|$.

We also found that the mean bubble rising speed is less than $|\mathbf{Q}|$ due to the trapping of bubbles by intense vortical regions. This decrease is about 33% at $\tau_b/\tau_k = |\mathbf{Q}|/v_k = 1$. A detailed study of this aspect will be reported in a separate publication.

Acknowledgements

This work is supported by the US Office of Naval Research through award N00014-91-J-1340. The computations were done at the Pittsburgh Supercomputing Center.

References

1. Squires, K.D. and Eaton, J.K.: 1991, *J. Fluid Mech.* **226**, 1.
2. Yeh, F. and Lei, U.: 1991, *Phys. Fluids A* **3**, 2571.
3. She, Z-S., Jackson, E., and Orszag, S.A.: 1990, *Nature* **344**, 226.
4. Brasseur, J.G. and Lin, W-Q.: 1991, in *Advances in Turbulence* **3**, Springer-Verlag, Heidelberg (Ed. Johansson and Alfredsson), pp3-12.
5. Ruetsch, G.R. and Maxey, M.R.: 1991, *Phys. Fluids A* **3**, 1587.
6. Chung, J.N. and Troutt, T.R.: 1988, *J. Fluid Mech.* **186**, 199.
7. Lazaro, B.J. and Lasheras, J.C.: 1989, *Phys. Fluids. A* **1**, 1035.
8. Wang, L-P., Maxey, M.R., Burton, T.D., and Stock, D.E.: 1992, *Phys. Fluids A* **4**, 1789.
9. Maxey, M.R. and Corrsin, S.: 1986, *J. Atmos. Sci.* **43**, 1112.
10. Maxey, M.R.: 1987, *Phys. Fluids* **30**, 1915.
11. Maxey, M.R.: 1987, *J. Fluid Mech.* **174**, 441.
12. Squires, K.D. and Eaton, J.K.: 1991, *Phys. Fluids A* **3**, 1169.
13. Wang, L-P. and Maxey, M.R.: 1992, 'Settling velocity and concentration distribution of heavy particles in homogeneous isotropic turbulence', Submitted to *J. Fluid Mech.*
14. Sridhar, G. and Katz, J.: 1992, *ASME Forum on Cavitation and Multiphase Flow*, Los Angeles, June 21-26. FED-Vol 135.

15. Lance, M. and Bataille, J.: 1991, *J. Fluid Mech.* **222**, 95-118.
16. Lance, M., Marie, J.L., and Bataille, J.: 1991, *ASME J. Fluids Eng.* **113**, 295-300.
17. Auton, T.R., Hunt, J.C.R., and Prud'Homme, M.: 1988, *J. Fluid Mech.* **197**, 241.
18. Balachandar, S. and Maxey, M.R.: 1989, *J. Comp. Phys.* **83**, 96.